

# Force Myography based Torque Estimation in Human Knee and Ankle Joints

Charlotte Marquardt<sup>\*‡</sup>, Arne Schulz<sup>\*</sup>, Miha Dežman<sup>\*</sup>, Gunther Kurz<sup>†</sup>, Thorsten Stein<sup>†</sup> and Tamim Asfour<sup>\*‡</sup>

**Abstract**—Online adaptation of exoskeleton control based on muscle activity sensing is a promising way to personalize exoskeletons based on user’s biosignals. While several electromyography (EMG) based methods have been shown to improve joint torque estimation, EMG sensors require direct skin contact and complex post-processing. In contrast, force myography (FMG) measures normal forces from changes in muscle volume due to muscle activity. We propose an FMG-based method to estimate knee and ankle joint torques by combining joint angles and velocities with muscle activity information. We learn a model for joint torque estimation using Gaussian process regression (GPR). The effectiveness of the proposed FMG-based method is validated on isokinetic motions performed by two subjects. The model is compared to a baseline model using only joint angle and velocity, as well as a model augmented by EMG data. The results show that integrating FMG into exoskeleton control improves the joint torque estimation for the ankle and knee and is therefore a promising way to improve adaptability to different exoskeleton users.

## I. INTRODUCTION

Lower limb exoskeletons are wearable devices designed to assist or augment mobility. While the design and control of these devices have traditionally focused on joint biomechanics, there is growing interest in incorporating muscle-level biomechanics for more effective interaction with the wearer’s musculoskeletal system. Incorporating muscle-level biomechanics into exoskeleton design and control has the potential to overcome some of the current limitations, such as lack of personalization in control, including the need to manually adjust control parameters for each user or track user fatigue or energy expenditure [1]. Muscle biomechanics research provides valuable data and insights to understand human movements and the function of the joints involved and can thus improve the robustness of exoskeleton control [2].

To incorporate muscle biomechanics into exoskeleton control, methods are needed to measure or estimate these biomechanics. Such methods should provide relevant biomechanical data in real-time during static and dynamic motion and must be compatible with the physical structure of the exoskeleton. During muscle activation, the muscle fibers are electrically stimulated resulting in a contraction of the muscle fibers and change of the muscle shape. Electromyography

(EMG) is a widely recognized approach to capture electrical effects of muscle activity [3]–[5]. However, ensuring high-quality EMG signals requires extensive filtering and signal post-processing. The signal quality can be negatively affected by several factors, including electrode positioning on the muscle, electrode skin contact, and the electrode displacement during muscle contraction. In contrast, force myography (FMG) detects the mechanical phenomena associated with muscle contraction rather than electrical effects, by measuring normal forces resulting from muscle volume change. Consequently, it does not require direct skin contact, precise sensor placement on the muscle and complex post-processing [6], [7]. It only requires contact between the body and the exoskeleton to measure the interaction forces between both. This allows the integration of force sensors into exoskeleton cuffs, making FMG-based control of exoskeletons a very promising technology.

In our previous work, we investigated the use of FMG for exoskeletons using barometric pressure-based FMG units [7]. This paper presents a deeper investigation of using FMG to estimate joint torques of the knee and ankle joint based on the combination of the joint angle and velocity with muscle activity. The introduction of muscle activity in the model supports the goal of bridging the gap between personalization and generalization of the exoskeleton control, as it allows for adapting the joint torque according to the user’s muscle activity. To do so, we learn a model for joint torque estimation using Gaussian process regression (GPR). We consider the proposed FMG-based approach for estimating joint torque



Fig. 1: The setup for isokinetic knee joint motion with a subject on the used IsoMed 2000 device.

This work has been supported by the Carl Zeiss Foundation through the JuBot project.

<sup>\*</sup>High Performance Humanoid Technologies Lab, Institute for Anthropomatics and Robotics, Karlsruhe Institute of Technology (KIT), Germany

<sup>†</sup>BioMotion Center, Institute of Sports and Sports Sciences, Karlsruhe Institute of Technology (KIT), Germany

<sup>‡</sup> Corresponding authors: {charlotte.marquardt, asfour}@kit.edu

an important initial step towards personalized exoskeleton control. We demonstrate the potential of the approach using data collected in a user study with two subjects performing isokinetic exercises, in which the velocity of the limb movement is maintained constant with varying resistance and muscle forces. We compared our model to a baseline model using only joint angle and velocity, as well as a model augmented by EMG data.

The paper is organized as follows. Section II discusses current related work while Section III describes the used model to estimate the joint torques, the conducted user study, the used sensor setup as well as the processing of the recorded signals. The quality of the torque estimation and its validation results are presented in Section IV and discussed in Section V. Section VI concludes the paper.

## II. RELATED WORK

Using multiple different sensing methods to capture muscle activity has created an opportunity to estimate human joint torque during exoskeleton usage. Previous work has explored a variety of EMG-driven methods for actuation and estimation of joint torques in exoskeleton control, and intention prediction [8]. Often, EMG methods are combined with neuromusculoskeletal (NMS) models, which accounts for the changes in joint angles and muscle dynamics and therefore improves the performance of human-robot cooperation control in exoskeletons [9]. The EMG with NMS performs best when calibrated in trials with high muscle activation. However, its combination with an artificial neural network (ANN) showed superior performance when trained in a diverse set of trials [10]. In ongoing work, a hybrid-ANN model incorporating physical features outperformed both the previous NMS and standard-ANN models in torque estimation [11]. Combinations with inertial sensors are also possible, allowing hybrid methods to combine inertial sensors and EMG-driven simulation to characterize the mechanics of the knee joint and muscle during walking [12]. The use of NMS models allows for personalization, as demonstrated through the person-specific NMS estimation of the biological torques of the ankle joint in real-time from measured EMG and joint angles [13]. Other EMG-based methods provide direct feedback for controlling the torque in exoskeletons or prostheses. Proportional myoelectric control directly uses the muscle activity amplitude to control the torque output of the exoskeleton [14]. Studies showed that users of a proportional myoelectric controlled ankle exoskeleton maintained their normal joint biomechanics [15], however the effect on metabolic cost was limited during walking both on a treadmill and outdoors [16], [17]. Moreover, these controllers measure only the resulting behavior of the muscle actions and thus do not fully capture the muscle and body mechanics [1]. In general, these results show the potential to integrate EMG signals, either directly or in advanced algorithms, to personalize joint torque estimation and torque control of exoskeletons.

On the other hand, FMG has been extensively and successfully investigated in various wearable applications such as

upper arm or hand motion classification and intention detection [18]–[21], lower limb gait phase or event detection [22], [23] and ankle position classification [24] often showing to outperform EMG-based methods. To estimate muscle forces a multisensory wearable system using ultrasound sensors was presented [25]. It combines a wearable ultrasound device and an inertial measurement unit (IMU) sensor to detect real-time muscle deformation and thickness changes caused by joint angle variations and achieves high accuracy during isometric contraction and shows a significant improvement in dynamic muscle force estimation. Sakr et al. [26] investigated the feasibility of using FMG signals from the lower arm to estimate multi-directional isometric hand force/torque. However, to the author’s knowledge, this approach has not been enhanced to estimate continuous isokinetic lower limb motion.

## III. METHODS

Accurate biomechanical models of joint kinematics in combination with normal muscle forces are difficult to obtain. To learn the relationship between kinematics and muscle force, we propose a Gaussian process regression (GPR) model. This section describes the model and the user study, including the sensor setup used to provide data for the training and validation of the model.

### A. GPR- for Joint Torque Estimation

GPR models are a kernel-based probabilistic and parametric supervised learning method for input-output mapping of empirical data that follows a joint Gaussian distribution [27]. In vector form, this can be described by

$$f(\mathbf{x}) \sim \mathcal{GP}(m(\mathbf{x}), k(\mathbf{x}, \mathbf{x}')), \quad (1)$$

where an observed outcome  $f$  is estimated from an input  $x$  by a Gaussian process with the mean function  $m$  and the covariance function  $k$ . Together with the error variance  $\sigma^2$ , they form hyperparameters optimized by maximizing the log marginal likelihood and minimizing the cross-validation loss. The mean function  $m$  is often used to incorporate prior knowledge and is commonly set to zero if no approximation model is known.

The observed joint torque  $T_J$  (which is equivalent to  $f(\mathbf{x})$  in Eq. (1)) is estimated using a radial basis function (RBF) as the covariance function of the GPR described as

$$k(\mathbf{x}, \mathbf{x}') = \exp\left(-\frac{1}{2}\|\mathbf{x} - \mathbf{x}'\|^2\right). \quad (2)$$

The input  $\mathbf{x}$  comes in three different configurations

$$\mathbf{x} = \begin{cases} (\theta_J, \omega_J)^T & \text{baseline} \\ (\theta_J, \omega_J, \mathbf{M}_{\text{EMG}})^T & \text{EMG} \\ (\theta_J, \omega_J, \mathbf{M}_{\text{FMG}})^T & \text{FMG} \end{cases} \quad (3)$$

consisting of the joint angle  $\theta_J$ , the joint angular velocity  $\omega_J$ , and the muscle signal  $\mathbf{M}$  obtained from either FMG or EMG signal which result in the corresponding estimated joint torques  $\tilde{T}_{J,\text{baseline}}$ ,  $\tilde{T}_{J,\text{FMG}}$  and  $\tilde{T}_{J,\text{EMG}}$ .

For each joint, the muscle signal  $\mathbf{M}$  was selected based on the primary muscles involved in the motion of that joint [28]:

$$\mathbf{M} = \begin{cases} (M_{TA}, M_{GM}, M_{GL}) & \text{ankle joint} \\ (M_{BF}, M_{RF}, M_{ST}, M_{VM}, M_{VL}) & \text{knee joint} \end{cases} \quad (4)$$

where  $M_{TA}$ ,  $M_{GM}$ ,  $M_{GL}$ ,  $M_{BF}$ ,  $M_{RF}$ ,  $M_{ST}$ ,  $M_{VM}$  and  $M_{VL}$  correspond to the muscular signals of the *tibialis anterior* (TA), *gastrocnemius medialis* (GM), *gastrocnemius lateralis* (GL), *biceps femoris* (BF), *rectus femoris* (RF), *semitendinosus* (ST), *vastus medialis* (VM) and *vastus lateralis* (VL). The effects of biarticular muscles, which influence the movements of multiple joints at the same time, have not been considered beyond the joints described in Eq. (4).

### B. User Study

To validate the model combining joint biomechanics and muscle signals in isokinetic motion, a user study was conducted in a controlled laboratory setting. In isokinetic motion, the velocity of the limb movement is maintained constant with varying muscle forces.

For this paper, two healthy adult subjects (one male, one female) were considered for the analysis. The experimental protocol was approved by the Karlsruhe Institute of Technology (KIT) Ethics Committee under the JuBot project. The subjects provided their informed consent in writing prior to the experiment and all methods were performed in accordance with the Declaration of Helsinki.

The user study was carried out using an IsoMed 2000 device, which allows isokinetic motion of the left ankle and knee joint in the sagittal plane (Fig. 1 and Fig. 2). The experiments were conducted in a sitting position on the IsoMed with a swinging leg/foot rest. For each joint, the subjects had a familiarization period of up to 10 minutes with the IsoMed device during which the maximum range of motion of the ankle and knee joints was also collected. The device's mechanical end stops were positioned to correspond with the user's maximum range of motion within their anatomical limits. Following this, the subjects performed two tasks in a random order:

- *Knee*: First, the knee joint was positioned at the maximum extension for initialization (Fig. 2a). Next, the subject performed a series of five swing motions including flexion and extension within their maximum active range of motion, maintaining a constant maximum angular velocity. These motions were carried out at four different angular velocities:  $60^\circ/s$ ,  $90^\circ/s$ ,  $120^\circ/s$ , and  $150^\circ/s$ . The initialization procedure and the five swing motions were repeated three times for each velocity, resulting in three recordings per angular velocity.
- *Ankle*: The ankle joint was first initialized in a position in which the foot was orthogonal to the shank (Fig. 2b). Next, the subject performed five swing motions including dorsi- and plantarflexion between the maximum angles of their active joint range. The initialization procedure and the five swing motions were repeated three times for velocities:  $30^\circ/s$ ,  $60^\circ/s$ ,  $90^\circ/s$  and  $120^\circ/s$ , resulting in three recordings per angular velocity.

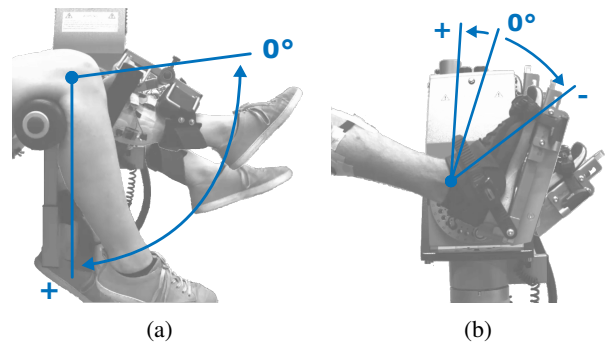


Fig. 2: Subject set-up on the IsoMed system for knee motion (a) and ankle motion (b) and the corresponding definition of the direction of the joint angle  $\theta_j$ .

For calibration purposes, FMG was initialized before accessing the IsoMed by standing upright and relaxed on both feet for approximately 10 seconds. Calibration measurements of the joint angle were conducted at each initial position  $\theta_j = 0^\circ$  as marked in Fig. 2.

### C. Sensor Setup

The used FMG sensor unit, which is described in [7], measures the normal force resulting from a change in volume and stiffness of the human muscle underneath the cuff during leg motion. The sensor unit comprises five barometric pressure sensors on a single printed circuit board (PCB), covered by a silicon dome. Variations in pressure detected by these sensors reflect changes in the forces applied to the silicon dome.

Eight FMG units and eight EMG electrode pairs were placed at anatomically relevant locations to measure the muscle activity of *RF*, *BF*, *ST*, *VM*, *VL*, *GM*, *GL* and *TA* as displayed in Fig. 3. The positions were determined based on EMG placement recommendations from SENIAM [29] combined with an assessment of real-time feedback from the EMG sensor. The two EMG electrodes were attached above and below the FMG sensor unit along the course of

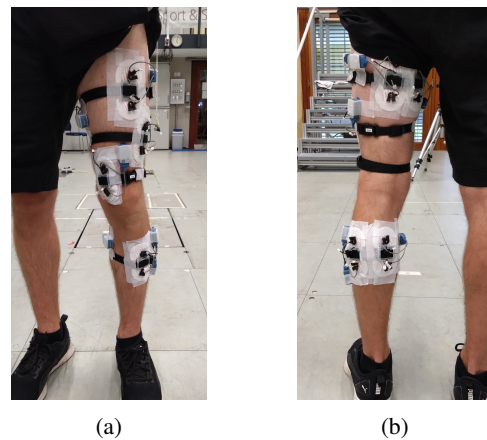


Fig. 3: EMG and FMG sensor positions on the front (a) and back (b) of the left leg.

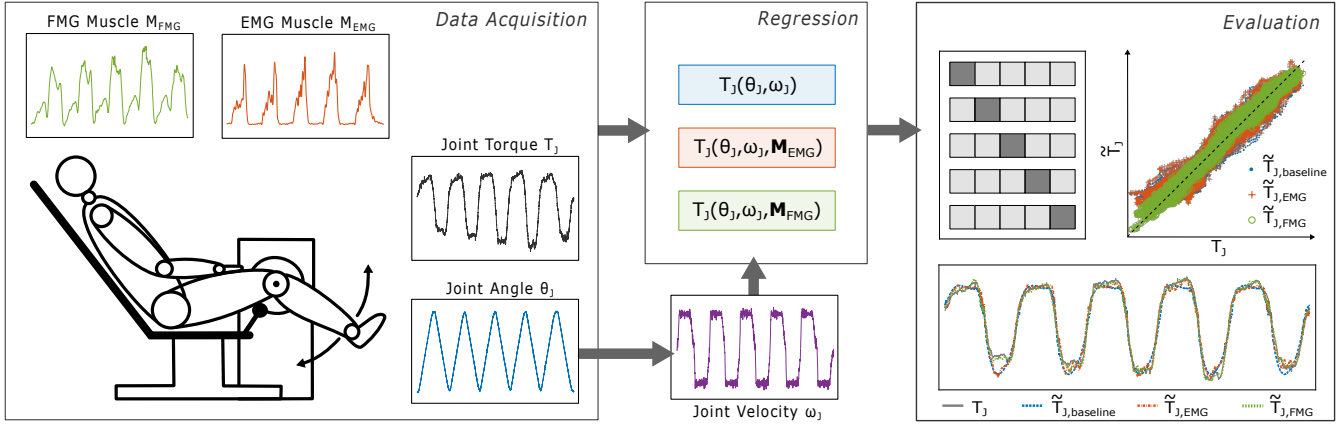


Fig. 4: Schematic representation of the torque estimation and validation process for a knee joint motion.

the muscle to ensure measurement at the same point on the muscle. In addition, the respective angular position  $\theta_J$  and torque of the joints  $T_J$  were recorded via the IsoMed device.

#### D. Signal Processing

A schematic overview of the entire torque estimation and validation process is given in Fig. 4.

The calibration of both, the FMG signal and the joint angle signal was performed using the mean values obtained from the calibration measurement. The amplitudes of the EMG signals are stochastic and the signal fluctuates rapidly around zero. Therefore, the signals were band-pass filtered between 20 Hz to 500 Hz, rectified and afterwards low-pass filtered at 6 Hz. All filters applied were fourth-order bi-directional Butterworth filters to achieve zero phase distortion. The angular joint velocity was derived from the joint angle. A second order Butterworth filter with a cutoff frequency of 20 Hz was applied bi-directionally before calculating the gradient. The segmentation of each complete motion including flexion and extension of the knee joint and dorsi- and plantarflexion of the ankle joint was performed based on the filtered joint angle to make it easier to recognize their extrema corresponding to the change in direction.

The FMG sensor units allow a maximum sampling rate of 200 Hz, while the joint angle, joint torque, and EMG signals were sampled at 2000 Hz. To align and concatenate all data, each dataset was linearly interpolated to an equidistant number of data points resulting in a down-sampling of the joint angle and EMG data to fit the FMG data. To ensure comparability, all data was normalized by variance and after regression the estimated joint torque was denormalized to its original scale.

The evaluation of the estimation results was based on 5-fold cross-validation. The variance and standard deviation of the model estimation were evaluated by mean-squared error (MSE) and root-mean-squared error (RMSE) respectively. A lower value of MSE and RMSE implies a higher accuracy of the GPR model.

## IV. RESULTS

The evaluation of the proposed approach based on GPR for estimating the joint torque included cross-validation to determine the quality of the method. The variance and standard deviation resulting from the cross-validation of the model are presented in Table I, while Fig. 5 shows the fit of the estimated versus the measured joint torque in all training and test data. The estimation results for an exemplary take from the user study are shown in Fig. 6.

Table I shows the variance and standard deviation of the 5-fold cross-validation for the joint torque estimation based on the MSE and RMSE respectively. Adding EMG information to the regression model only leads to smaller improvements, while the MSE and RMSE improve by about 88 % and 66 % for the ankle joint and by about 79 % and 54 % for the knee joint, respectively, when integrating muscular information measured via FMG instead of EMG.

TABLE I: 5-fold cross-validation results

	Ankle		Knee	
	MSE	RMSE	MSE	RMSE
baseline	0.0906	0.3009	0.0428	0.2070
EMG	0.0502	0.2240	0.0312	0.1766
FMG	0.0105	0.1026	0.0092	0.0957

Values are based on the normalized data.

The direct fit of the estimated versus the measured joint torque in all training and test data is demonstrated in Fig. 5. The diagonal 45° line shows an optimal fit between both torques; the closer the data points are, the better the estimation. The presented RMSE quantifies the visual data, showing that FMG reduces the error between the baseline and the estimation model more effectively than EMG. The quality of the fit of the estimation model improves when adding information about muscle activity, with FMG outperforming EMG. While in the baseline model the RMSE of the estimated torque  $\tilde{T}_{J,\text{baseline}}$  is about 5 % to 7 % of the measured joint torque  $T_J$ , it is reduced to 4 % to 5 % and 2 % to 3 %



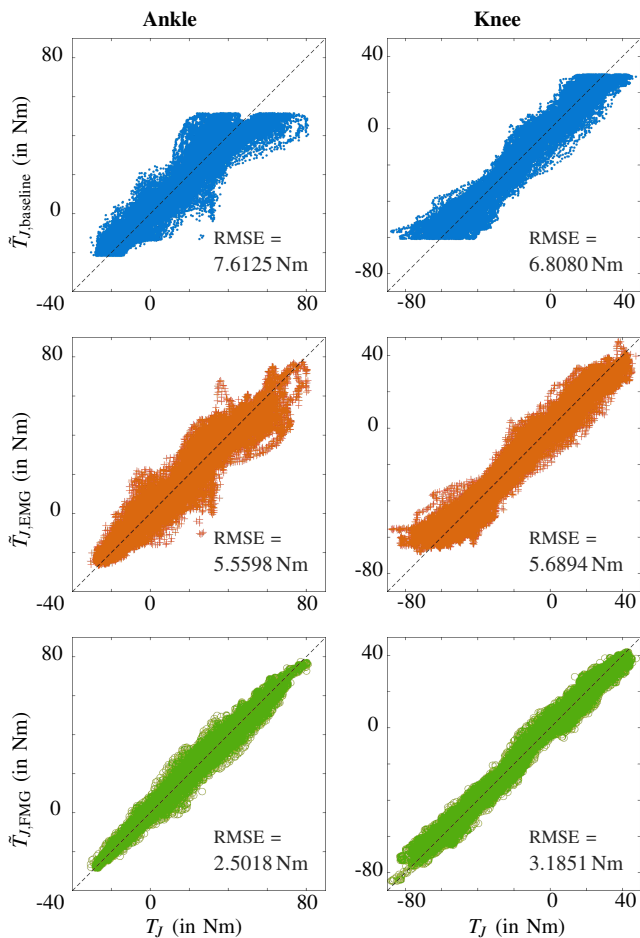


Fig. 5: Measured vs. estimated torque for all three model configurations, baseline (top), EMG (middle) and FMG (bottom), for both the ankle (left) and the knee (right) joint. The graph displays the complete data used for training and validation of the GPR models.

for the EMG- and FMG-based model ( $\tilde{T}_{J,EMG}$  and  $\tilde{T}_{J,FMG}$ ) respectively.

An exemplary joint torque estimation of time series data from one subject is presented in Fig. 6. It shows the estimated and measured joint torque during isokinetic motion at  $60^\circ/s$  over time for the three model configurations separately for the ankle (Fig. 6a) and knee (Fig. 6b) joint. The baseline model, depending only on joint angle and velocity, shows a consistent estimation that does not vary with the torque amplitude. Adding muscle signals to the model improves the adaptability concerning the trajectory. However, the EMG-based model still shows inaccuracies in the peak torques, while the FMG-based model follows each variation of the joint torque trajectory more closely.

## V. DISCUSSION

This work introduces a FMG-based approach to estimate torques in the knee and ankle joints. It utilizes joint angles and velocities along with muscle activity, modeled using GPR. The effectiveness of this FMG-based method

is validated through a study involving two subjects and is compared with a baseline model that only uses joint angle and velocity, as well as a model based on EMG. The FMG-based approach offers promising results that include lower variance and standard deviation compared to the baseline and EMG-based model, as well as greater adaptability to variations in joint torque that an estimation based only on joint angle and velocity cannot take into account.

Fig. 6 shows that the baseline model produces a very similar trajectory for each repetition, while the EMG- and FMG-based models vary in amplitude according to the measured muscle activity and thus the varying torque amplitude. This difference is also quantified by the RMSE, which decreases for the FMG-based model both in cross-validation and in general for the complete training and validation set. However, the EMG-based torque estimate failed to predict the first and fourth peaks, whereas the FMG-based model estimate accurately represented all peaks. This discrepancy in the EMG estimate is likely due to building models using data from two subjects and then using them to estimate torque for only one subject. The better performance of the FMG estimate suggests that the FMG method may have better generalization across subjects compared to EMG, which is an interesting point for future investigation.

In comparison, 5-fold cross-validation allowed the model to be tested on data it has not been trained on. Although the MSE and RMSE were higher than when the model was directly estimated using data it was trained on, the estimation of joint torque slightly improved after integrating EMG in the model and notably improved after integration of FMG. However, the proposed method was only trained and validated on two subjects, whose data was divided into five parts for validation. To address this limitation, future studies will include a larger and more diverse group of subjects. This will enable better generalization of the findings and validation of the model across a wider range of people. It will enable evaluation not only based on randomly chosen cross-validation results but also on unknown subjects. In addition, it will allow further investigation into inter- and intra-subject variability of the estimation data.

The current approach uses a fully data-driven method with a complex-to-interpret GPR model. Future research aims to incorporate additional prior knowledge into the GPR model, drawing inspiration from biomechanical models or exploring other more interpretable model options. This approach can potentially reduce the amount of data required for training such a model and enable to better understand the effect of each input signal on the model output.

In this study, the focus was solely on the isokinetic motion in the sagittal plane. The purpose of future research is to encompass a range of activities of daily living to confirm the findings in a spectrum of combined motions and to determine the comprehensibility of muscular signals during motions including multiple directions.

In the future, when using an exoskeleton, the forces used to move it can interfere with measuring muscle activity using FMG due to potential disturbance forces caused by

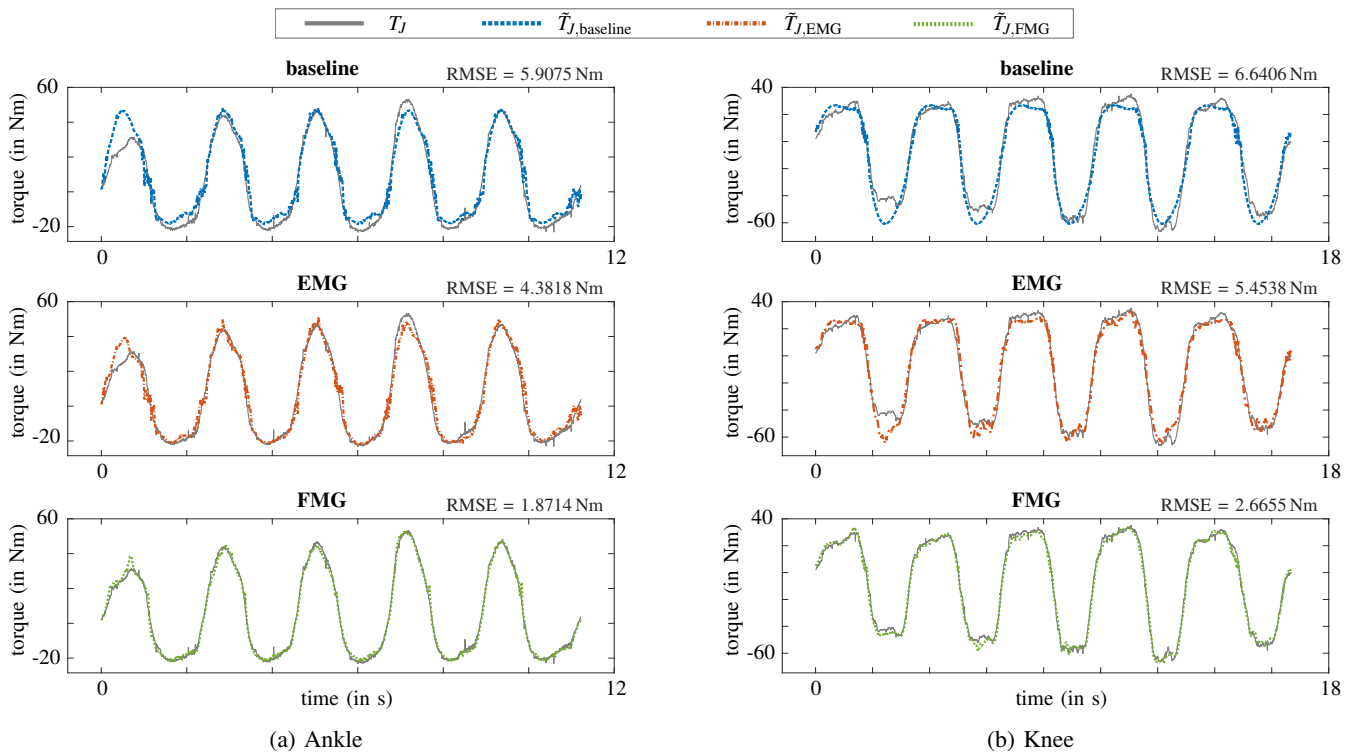


Fig. 6: Measured and estimated torque over time for all three model configurations, baseline (top), EMG (middle) and FMG (bottom) of both the ankle (a) and knee (b) joint. The exemplary data was taken from one recording of the isokinetic motion at  $60^\circ/\text{s}$  of one subject.

the interaction between the exoskeleton and the user. Even in this laboratory setup, we cannot completely rule out the possibility that other parasitic forces resulting from co-contraction or external perturbations may interfere with the normal muscle force measurements. In our previous work, we have shown how motion restrictions due to an ankle exoskeleton can impact FMG sensor signals [30]. Further research will reveal the extent to which actuation can influence FMG-based torque estimation and control.

The results emphasize that FMG technology offers a promising alternative to EMG technology for the development of more versatile assistive exoskeleton, but more research into its performance and applicability in exoskeleton control is required.

## VI. CONCLUSION

Incorporation of muscle activity signals is an important approach for real-time personalization of exoskeleton control. We proposed a FMG-based approach to estimate knee and ankle joint torques using joint angles, velocities, and muscle activity and a GPR model. The validation of the effectiveness of the torque estimation based on FMG was carried out through a user study involving two subjects performing isokinetic ankle and knee motion. Comparative analysis was performed against a baseline model that only used joint angle and velocity data, as well as a model augmented with muscle activity signals obtained by EMG. The results indicate that the integration of FMG into wearable devices

has the potential to improve the adaptability across diverse user profiles. Furthermore, our work underscores FMG technology as a promising alternative to EMG for developing control methods for adaptive assistive exoskeleton devices. This highlights the potential of FMG-based models of bridging the gap between personalization and generalization in exoskeleton control by facilitating torque adaptation based on individual biosignals, thereby eliminating the need for manual adjustments.

## REFERENCES

- [1] Z. S. Mahdian, H. Wang, M. I. M. Refai, G. Durandau, M. Sartori, and M. K. MacLean, "Tapping Into Skeletal Muscle Biomechanics for Design and Control of Lower Limb Exoskeletons: A Narrative Review," *Journal of Applied Biomechanics*, vol. 39, no. 5, pp. 318 – 333, 2023.
- [2] J. Wang, D. Wu, Y. Gao, X. Wang, X. Li, G. Xu, and W. Dong, "Integral Real-time Locomotion Mode Recognition Based on GA-CNN for Lower Limb Exoskeleton," *Journal of Bionic Engineering*, Jul. 2022.
- [3] C. D. Joshi, U. Lahiri, and N. V. Thakor, "Classification of gait phases from lower limb EMG: Application to exoskeleton orthosis," in *2013 IEEE Point-of-Care Healthcare Technologies (PHT)*, Jan. 2013, pp. 228–231, ISSN: 2377-5270.
- [4] J. Taborri, E. Palermo, S. Rossi, and P. Cappa, "Gait Partitioning Methods: A Systematic Review," *Sensors*, vol. 16, no. 1, 2016.
- [5] S. Jiang, P. Kang, X. Song, B. Lo, and P. B. Shull, "Emerging Wearable Interfaces and Algorithms for Hand Gesture Recognition: A Survey," *IEEE Reviews in Biomedical Engineering*, pp. 1–1, 2021.
- [6] C. Castellini and V. Ravindra, "A wearable low-cost device based upon Force-Sensing Resistors to detect single-finger forces," in *5th IEEE RAS/EMBS International Conference on Biomedical Robotics*

- and *Biomechatronics*. Sao Paulo, Brazil: IEEE, Aug. 2014, pp. 199–203.
- [7] C. Marquardt, P. Weiner, M. Dežman, and T. Asfour, “Embedded barometric pressure sensor unit for force myography in exoskeletons,” in *IEEE/RAS International Conference on Humanoid Robots (Humanoids)*, Ginowan, Okinawa, Japan, 2022, pp. 67–73.
- [8] D. Xu, Q. Wu, and Y. Zhu, “Development of a sEMG-Based Joint Torque Estimation Strategy Using Hill-Type Muscle Model and Neural Network,” *Journal of Medical and Biological Engineering*, vol. 41, no. 1, pp. 34–44, Feb. 2021.
- [9] D. Ao, R. Song, and J. Gao, “Movement Performance of Human–Robot Cooperation Control Based on EMG-Driven Hill-Type and Proportional Models for an Ankle Power-Assist Exoskeleton Robot,” *IEEE Transactions on Neural Systems and Rehabilitation Engineering*, vol. 25, no. 8, pp. 1125–1134, Aug. 2017.
- [10] L. Zhang, Z. Li, Y. Hu, C. Smith, E. M. G. Farewik, and R. Wang, “Ankle Joint Torque Estimation Using an EMG-Driven Neuromusculoskeletal Model and an Artificial Neural Network Model,” *IEEE Transactions on Automation Science and Engineering*, vol. 18, no. 2, pp. 564–573, Apr. 2021.
- [11] L. Zhang, X. Zhu, E. M. Gutierrez-Farewik, and R. Wang, “Ankle Joint Torque Prediction Using an NMS Solver Informed-ANN Model and Transfer Learning,” *IEEE Journal of Biomedical and Health Informatics*, vol. 26, no. 12, pp. 5895–5906, Dec. 2022.
- [12] R. D. Gurchiek, N. Donahue, N. M. Fiorentino, and R. S. McGinnis, “Wearables-Only Analysis of Muscle and Joint Mechanics: An EMG-Driven Approach,” *IEEE Transactions on Biomedical Engineering*, vol. 69, no. 2, pp. 580–589, Feb. 2022.
- [13] G. Durandau, W. F. Rampeltshammer, H. v. d. Kooij, and M. Sartori, “Neuromechanical Model-Based Adaptive Control of Bilateral Ankle Exoskeletons: Biological Joint Torque and Electromyogram Reduction Across Walking Conditions,” *IEEE Transactions on Robotics*, vol. 38, no. 3, pp. 1380–1394, Jun. 2022.
- [14] R. L. Hybart and D. P. Ferris, “Preliminary Validation of Proportional Myoelectric Control of A Commercially Available Robotic Ankle Exoskeleton,” in *2022 International Conference on Rehabilitation Robotics (ICORR)*. Rotterdam, Netherlands: IEEE, Jul. 2022, pp. 1–5.
- [15] —, “Neuromechanical Adaptation to Walking With Electromechanical Ankle Exoskeletons Under Proportional Myoelectric Control,” *IEEE Open Journal of Engineering in Medicine and Biology*, vol. 4, pp. 119–128, 2023.
- [16] R. Hybart, K. S. Villancio-Wolter, and D. P. Ferris, “Metabolic cost of walking with electromechanical ankle exoskeletons under proportional myoelectric control on a treadmill and outdoors,” *PeerJ*, vol. 11, p. e15775, Jul. 2023.
- [17] R. Hybart and D. Ferris, “Gait variability of outdoor vs treadmill walking with bilateral robotic ankle exoskeletons under proportional myoelectric control,” *PLOS ONE*, vol. 18, no. 11, p. e0294241, Nov. 2023.
- [18] M. R. U. Islam and S. Bai, “Effective Multi-Mode Grasping Assistance Control of a Soft Hand Exoskeleton Using Force Myography,” *Frontiers in Robotics and AI*, vol. 7, p. 139, 2020.
- [19] Z. G. Xiao and C. Menon, “Performance of forearm FMG and sEMG for estimating elbow, forearm and wrist positions,” *Journal of Bionic Engineering*, vol. 14, no. 2, pp. 284–295, 2017.
- [20] X. Jiang, L.-K. Merhi, Z. G. Xiao, and C. Menon, “Exploration of Force Myography and surface Electromyography in hand gesture classification,” *Medical Engineering & Physics*, vol. 41, pp. 63–73, Mar. 2017.
- [21] A. Belyea, K. Englehart, and E. Scheme, “FMG Versus EMG: A Comparison of Usability for Real-Time Pattern Recognition Based Control,” *IEEE Transactions on Biomedical Engineering*, vol. 66, no. 11, pp. 3098–3104, Nov. 2019.
- [22] M. R. Islam and S. Bai, “A novel approach of FMG sensors distribution leading to subject independent approach for effective and efficient detection of forearm dynamic movements,” *Biomedical Engineering Advances*, vol. 4, p. 100062, 2022.
- [23] X. Jiang, H. T. Chu, Z. G. Xiao, L.-K. Merhi, and C. Menon, “Ankle positions classification using force myography: An exploratory investigation,” in *2016 IEEE Healthcare Innovation Point-Of-Care Technologies Conference (HI-POCT)*, Nov. 2016, pp. 29–32.
- [24] X. Jiang, L. Tory, M. Khoshnam, K. Chu, and C. Menon, “Exploration of Gait Parameters Affecting the Accuracy of Force Myography-Based Gait Phase Detection,” in *2018 7th IEEE International Conference on Biomedical Robotics and Biomechatronics (Biorob)*, Aug. 2018, pp. 1205–1210, iSSN: 2155-1782.
- [25] Y. Lu, Y. Cao, Y. Chen, H. Li, W. Li, H. Du, S. Zhang, and S. Sun, “Investigation of a wearable piezoelectric-IMU multi-modal sensing system for real-time muscle force estimation,” *Smart Materials and Structures*, vol. 32, no. 6, p. 065013, 2023, publisher: IOP Publishing.
- [26] M. Sakr, X. Jiang, and C. Menon, “Estimation of User-Applied Isometric Force/Torque Using Upper Extremity Force Myography,” *Frontiers in Robotics and AI*, vol. 6, p. 120, Nov. 2019.
- [27] C. E. Rasmussen and Christopher K. I. Williams, *Gaussian process for machine learning*. London, England: The MIT Press, 2006, oCLC: 999818656.
- [28] D. A. Neumann and E. E. Rowan, *Kinesiology of the musculoskeletal system: foundations for physical rehabilitation*, 1st ed. St. Louis: Mosby, 2002, oCLC: 992214437.
- [29] H. J. Hermens, B. Freriks, R. Merletti, D. Stegeman, J. Blok, G. Rau, C. Disselhorst-Klug, and G. Hägg, “Seniam,” 1999, publisher: Roessingh Research and Development. [Online]. Available: <http://seniam.org/>
- [30] C. Marquardt, M. Dežman, and T. Asfour, “Influence of motion restrictions in an ankle exoskeleton on force myography in straight and curve walking,” in *IEEE/RAS/EMBS International Conference on Biomedical Robotics and Biomechatronics (BioRob)*, Heidelberg, Germany, September 2024.